Reduction of the Mn Cluster of the Water-Oxidizing Enzyme by Nitric Oxide: Formation of an S_{-2} State†

Gert Schansker,‡,§ Charilaos Goussias,*,|| Vasili Petrouleas,‡ and A. William Rutherford||

Institute of Materials Science, NCSR "Demokritos", 15310 Aghia Paraskevi, Athens, Greece, and Service de Bioénergétique, URA 2096 CNRS, CEA Saclay, 91191 Gif-sur-Yvette, France

Received October 30, 2001; Revised Manuscript Received January 14, 2002

ABSTRACT: The manganese cluster of the oxygen-evolving enzyme of photosystem II is chemically reduced upon interaction with nitric oxide at −30 °C. The state formed gives rise to an $S = {}^1/_2$ multiline EPR signal [Goussias, Ch., Ioannidis, N., and Petrouleas, V. (1997) *Biochemistry 36*, 9261] that is attributed to a Mn(II)−Mn(III) dimer [Sarrou, J., Ioannidis, N., Deligiannakis, Y., and Petrouleas, V. (1998) *Biochemistry 37*, 3581]. In this work, we sought to establish whether the state could be assigned to a specific, reduced S state by using flash oxymetry, chlorophyll *a* fluorescence, and electron paramagnetic resonance spectroscopy. With the Joliot-type O_2 electrode, the first maximum of oxygen evolution was observed on the sixth or seventh flash. Three saturating preflashes were required to convert the flash pattern characteristic of NO-reduced samples to that of the untreated control (i.e., O_2 evolution maximum on the third flash). Measurements of the S state-dependent level of chlorophyll fluorescence in NO-treated PSII showed a three-flash downshift compared to untreated controls. In the EPR study, the maximum S_2 multiline EPR signal was observed after the fourth flash. The results from all three methods are consistent with the Mn cluster being in a redox state corresponding to an S_{-2} state in a majority of centers after treatment with NO. We were unable to generate the Mn(II)−Mn(III) multiline signal using hydrazine as a reductant; it appears that the valence distribution and possibly the structure of the Mn cluster in the S_{-2} state are dependent on the nature of the reductant that is used.

PSII[1] is a large, multisubunit protein, located in the thylakoid membranes of higher-plant chloroplasts and in cyanobacteria. It catalyzes the light-driven reduction of a plastoquinone molecule, using water as the source of the required electrons and releasing molecular oxygen. The catalytic site of water oxidation is believed to contain a tetranuclear Mn cluster (with one calcium cation and at least one chloride anion), which undergoes a series of four one-electron oxidation transitions, cycling through five distinct oxidation states, designated S_0−S_4 (for reviews, see refs *1* and *2*). This is necessary, since the oxidation of two water molecules requires four oxidizing equivalents. Dark-adapted material contains predominantly the S_1 state. The S_0−S_1 and S_1−S_2 transitions correspond to the oxidation of Mn ions, while it is still under debate if the S_2−S_3 transition is associated with an oxidation of the cluster or of a ligand to the cluster (*3*, *4*). The S_4 state spontaneously decays to the S_0 state, with the simultaneous release of molecular oxygen.

EPR spectroscopy has been instrumental in characterizing the S states. The S_2 state exhibits two distinct signals, a multiline signal, centered at $g = 2$ (*5*) and an alternate signal at $g = 4.1$ (*6*−*8*). The multiline EPR signal is attributed to a ground state with spin $S = {}^1/_2$, probably due to two antiferromagnetically coupled Mn(III) and Mn(IV) ions within the tetramer, while the $g = 4.1$ signal has been attributed to a spin $S = {}^5/_2$ state of the tetrameric Mn cluster (*9*, *10*). The S_0 signal, which was expected to give rise to a half-integer spin state, remained undetected for years, until it was discovered that a low concentration of methanol rendered it detectable (*11*−*13*). Low-field EPR signals in both perpendicular and parallel modes have been assigned to the S_3 state (*14*, *15*).

The Mn cluster is assembled in apo-PSII by a light-driven, stepwise reaction known as photoactivation, which involves the binding of Mn^{2+} ions, and their oxidation. The assembly is characterized by two distinct, light-driven steps, separated by a dark interval. On the first light-dependent step, a Mn^{2+} ion binds to the PSII reaction center protein and is photo-oxidized with a high quantum yield. The dark interval is associated with the binding of a calcium ion, prior to a second light-driven step, which involves the binding and photo-oxidation of a second Mn^{2+} ion. The two remaining Mn^{2+} ions subsequently bind in a kinetically unresolved manner. The second light-driven step occurs with a low quantum yield, and subsequent redox intermediates have not been

† This work was supported by TMR Network Grant ERBF-BICT983497. Ch.G. is supported by a Marie Curie individual fellowship (MCFI-2000-00611).

* To whom correspondence should be addressed. Telephone: +33 1 69088657. Fax: +33 1 69088717. E-mail: haris314@yahoo.com.

‡ NCSR "Demokritos".

§ Present address: Laboratory of Bioenergetics, University of Geneva, Geneva, Switzerland.

|| CEA Saclay.

[1] Abbreviations: PSII, photosystem II; EPR, electron paramagnetic resonance; Tyr_D, redox-active tyrosine 160 on the D2 polypeptide of PSII; Tyr_Z, redox-active tyrosine 161 on the D1 polypeptide of PSII, electron donor to P680; chl, chlorophyll; MES, morpholineethanesulfonic acid; P-p-BQ, phenyl-*p*-benzoquinone; DMSO, dimethyl sulfoxide; EDTA, ethylenediaminotetraacetic acid.

10.1021/bi015903z CCC: $22.00
Published on Web 02/06/2002

isolated and studied (*16*, *17*). It is possible that chemical reduction of the functional Mn cluster may produce states that correspond to redox intermediates during the assembly of the Mn cluster.

Reduced forms of the Mn cluster corresponding to S states more reduced than S_0 have been reported. Reductants such as hydrazine or hydroxylamine have been used to generate the S_{-1}, S_{-2}, and S_{-3} states with good yields, although the characterization of these states was limited to O_2 electrode studies (*18*). There are few EPR studies on the reduced S states reported in the literature (*19*−*22*). One example is the report of the appearance of a hexa-aquo manganese spectrum in hydroquinone-reduced PSII (*19*), which could not be removed by a chelator, but could be diminished by illumination at 4 °C in the presence of Ca^{2+}. This (apparently bound) Mn^{2+} ion may correspond to a first photoactivation step, and represent an over-reduced S state.

A multiline EPR signal arises from the very slow interaction of NO with photosystem II at −30 °C (*20*). The state exhibiting this signal seems to require a specific incubation at this temperature. The EPR signal is lost after a brief incubation at room temperature, but it reappears after a relatively brief incubation (approximately 30 min) at −30 °C, even in the absence of NO. The EPR spectrum has been assigned to the ground state of a magnetically isolated Mn(II)−Mn(III) dimer (*21*), a fact that implied that NO acts as a reductant. The action of NO as a reductant was also demonstrated in Mn catalase (*23*). The time course of the reduction procedure in PSII indicated that the Mn(II)−Mn(III) state forms after reduction to the S_{-1} state (*22*). The state was tentatively assigned to the S_{-2} state, but lower states or a modified S_{-1} state could not be ruled out. In the study presented here, we attempt to assign this reduced form of the Mn cluster to a specific S state using flash oxymetry, chlorophyll fluorescence, and EPR spectroscopy.

EXPERIMENTAL PROCEDURES

PSII-enriched membranes were isolated from market spinach using standard protocols (*24*, *25*) and stored in liquid nitrogen, in a buffer solution containing 0.4 M sucrose, 15 mM NaCl, and 40 mM MES (pH 6.5). The chlorophyll concentration of samples was 3 mg/mL for the EPR samples. In all EPR samples, 50 μM EDTA was added before the NO treatment. This concentration of EDTA was sufficient to scavenge the small percentage of free Mn^{2+} (5−15% of the total, as estimated from the hexa-aquo manganese EPR spectrum), which was invariably released during the pumping process, and resulted in a clean baseline. However, this EDTA concentration is too low to scavenge the Mn^{2+} that would be released from a higher proportion of centers. Thus, such chemically damaged samples could still be identified.

P-p-BQ [dissolved in methanol, final methanol concentration of 1% (v/v)] was used as an exogenous electron acceptor in EPR samples. It was added before the NO treatment, as it was found that after the incubation and pumping, the material becomes rather sensitive to manipulations (such as stirring, dilution, centrifugation, and transfer under aerobic conditions).

Nitric oxide (99.5%) was supplied by Messer-Griesheim Co. Pure NO or a mixture of NO and nitrogen was added to dark-adapted PSII membranes (0 °C) anaerobically and directly into the EPR tube, using a Hamilton gastight syringe and Teflon tubing. Typical concentrations were 0.6 or 2 mM NO. The EPR tube was subsequently sealed using a rubber septum. Incubation at −30 °C was carried out in a freezer. The maximum Mn(II)−Mn(III) multiline signal was obtained after incubation for 18 h at −30 °C. For samples treated with 2 mM NO, 80−90% of the signal could be observed after only 4 h at −30 °C. Removal of free NO after maximum signal generation was performed by pumping, using a rotary pump at 0 °C. Care was taken so that the vacuum in the vacuum manifold was never below 10^{-2} mbar.

All samples for the oxygen evolution or fluorescence measurements were monitored by EPR for intactness, optimal Mn(II)−Mn(III) multiline generation, and complete removal of free NO. The material was taken from the EPR tube, diluted, and transferred under anaerobic conditions to the appropriate cuvette. All sample incubations and handling were performed under a dim green light. It was found that samples that were left overnight at −30 °C with 2 mM NO were more sensitive to manipulation. Incubation with NO was therefore limited to 4−6 h, at the cost of a somewhat decreased (by 10−20%) Mn(II)−Mn(III) multiline signal amplitude.

The flash oxygen measurements were carried out using an O_2 electrode built at the laboratory of I. Vass (Biological Research Center, Szeged, Hungary). The electrode was operated at a polarization voltage of 650 mV. The chlorophyll concentration was 1 mg/mL, and the measurements were performed in the presence of 50 mM KCl. Samples were dark-adapted for 3 min on the oxygen electrode before the measurement was started. The flash frequency for both the preflashes and the flash series was 1 Hz. Saturating flashes for the material measured on the O_2 electrode were performed with an EG&G FX-1248 xenon flash lamp at room temperature (18−20 °C). Electron acceptors were not used, as they interact with the polarized electrode. This is taken into account by the instrument software as an extra fitting parameter, which corrects for the number of PSII reaction centers that are closed after each flash, as a consequence of an empty Q_B site.

Fluorescence measurements were performed on a home-built chlorophyll fluorescence apparatus based on the design described in ref *26*. Saturating, single-turnover flashes were produced by a xenon lamp (EG&G FX-1248) shielded by a 1 mm Schott KG5 filter. Photosynthetic material was flashed at room temperature (18−20 °C). The time interval between the flashes was 100 ms. Fluorescence levels were recorded using low-intensity flash illumination by an array of eight Hewlett-Packard HLMA-CH00 light-emitting diodes. The fluorescence intensity was measured using a photodiode (Hamamatsu S2744-08) shielded by a 1 mm Schott RG695 cutoff filter. The collected data were converted using a 16-bit AD7885 analog-to-digital converter. The computer interface card was also homemade. The measurements were controlled by software written by L. Szass (Biological Research Center). Samples were diluted to a concentration of 10 μg of Chl/mL in a medium containing 0.4 M sucrose, 15 mM NaCl, and 40 mM MES (pH 6.5). To minimize limitations on the acceptor side of PSII, all fluorescence measurements were performed in the presence of 100 μM ferricyanide as an electron acceptor. Under our conditions, the miss factor was around 8%. At a flash frequency of 10

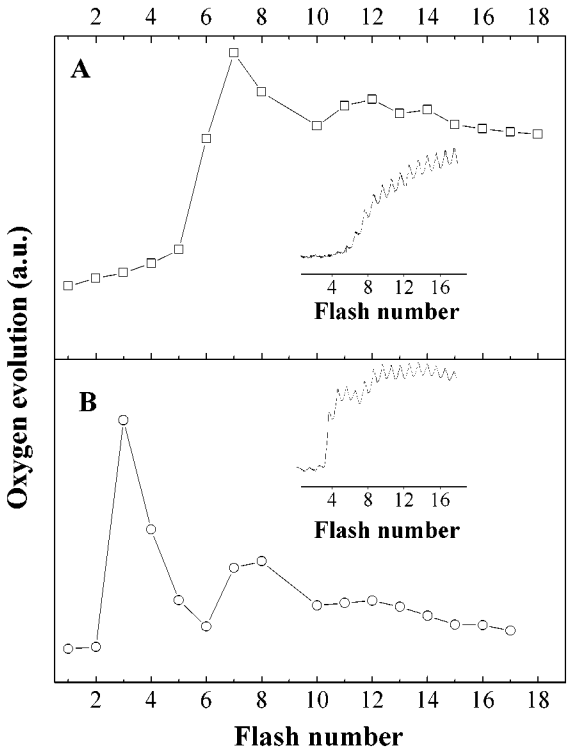

FIGURE 1: Oxygen oscillation patterns of PSII-enriched membranes from (A) NO-treated material displaying the Mn(II)−Mn(III) multiline EPR signal and (B) a control sample. The insets in both cases show raw data.

Hz, the added ferricyanide is not able to keep the plastoquinone pool in the oxidized state. Since oxidized plastoquinone is a strong fluorescence quencher in photosystem II membranes (see ref *27*), reduction of the plastoquinone pool causes an increase in the fluorescence level. As a consequence, the period 4 oscillations can be seen on a sigmoid background. The sigmoid over sequences of five flashes was approximated by line segments.

Electron paramagnetic resonance spectroscopy was performed using a Bruker ER-300 spectrometer, equipped with an Oxford ESR 9 cryostat, a Hewlett-Packard 5350B frequency counter, and a Bruker 035M NMR gaussmeter. Flash illumination of the EPR samples was performed with a Spectra Physics GCR-230-10 Nd:YAG laser (532 nm, 550 mJ, 8 ns pulse) at room temperature. The flashing frequency was 1 Hz. Illumination at 200 K was performed in an ethanol/solid CO_2 bath in an unsilvered dewar flask, using a 300 W projector lamp.

RESULTS

Flash Oxymetry. PSII-enriched membranes were treated with 0.6 or 2 mM NO and were incubated at −30 °C, and the Mn(II)−Mn(III) EPR signal was monitored. The material was subsequently pumped to remove free NO and diluted to a concentration of 1 mg of Chl/mL using a degassed buffer. The material was then transferred in the dark (under anaerobic conditions) to the O_2 electrode. In Figure 1, a sample treated with NO is compared with a control sample. The raw data are presented as insets of the derived oxygen patterns. The figure shows that PSII is still capable of oxygen evolution when reduced after treatment with NO. The figure also shows that in the NO-treated sample the first peak of O_2 evolution is shifted from flash 3 (i.e., in which the starting state was mainly S_1) to flash 6/7 (i.e., in which the starting state was S_{-2} or S_{-3}). Under the conditions of these measurements, a miss factor of 15−20% was calculated. This miss factor, which was obtained for control experiments using the O_2 electrode software, is larger than expected and is presumably a characteristic of the setup that is used.

When one starts with an S_{-2} state, such a miss factor predicts that O_2 evolution should be observed on the sixth and seventh flash, and the O_2 evolution should be higher on the seventh. Similarly, starting from S_{-3}, one would expect O_2 evolution to appear on the seventh and eighth flashes. It is clear from the data that the S_{-2} state is therefore more likely to be the dominant state produced by the NO treatment.

In some experiments, one to four preflashes were given followed by a period of dark adaptation prior to the assessment of the O_2 evolution induced by the flash train. It was found that each preflash resulted in a corresponding decrease in the number of flashes required for the first maximum in O_2 evolution (not shown). After four preflashes, however, no further reduction occurred in the number of flashes required for the first maximum of O_2 production. This indicates that the states formed by the first three preflashes are stable in the dark, while four preflashes generate a state that decays back to its previous redox state. This observation fits well with the majority of the centers being in the S_{-2} state after reduction with NO: the state generated by four preflashes is expected to be S_2 which decays back to S_1 in the dark, while the S_{-1}, S_0, and S_1 states are all stable in the dark.

In some samples, O_2 evolution was detected after the first flash (not shown). This oxygen production was eliminated by addition of catalase. There seemed to be no relationship between this first flash O_2 burst and the subsequent pattern of O_2 evolution. Oxygen production on the first flash was also sometimes observed in samples incubated for short times with NO even though the final reduction state had not been achieved and none of the Mn(II)−Mn(III) state had been formed as determined by EPR. It is thus clear that this phenomenon is not related to the state characterized by the Mn(II)−Mn(III) EPR signal.

EPR Measurements. In the EPR measurements, the NO-treated material was illuminated with a variable number of saturating laser flashes and the appearance of the known EPR signals of the S_2 state was monitored. Electron transfer out of the reaction center in PSII-enriched membrane preparations is usually less than optimal due to damage around Q_B, and the small size of the plastoquinone pool. It is therefore important that an exogenous quinone electron acceptor be used to ensure that the turnover at each flash is optimal. The solubility of P-p-BQ in water is too low to allow for a convenient stock solution; therefore, an organic solvent has to be used. As the presence of alcohols is known to affect the manganese EPR signals from the water-oxidizing enzyme (*11*, *12*, *28*), a study of the effect of solvents on the Mn(II)−Mn(III) signal was carried out. In Figure 2, we show the Mn(II)−Mn(III) spectra obtained after incubation for 18 h at −30 °C and the removal of free NO, without the addition of an organic solvent (Figure 2A), in the presence of 1% methanol (Figure 2B; see also ref *22*), 1% DMSO (Figure 2C), or 1% ethanol (Figure 2D). As in the case of the S_2 multiline EPR signal, one observes slight shifts of the peak

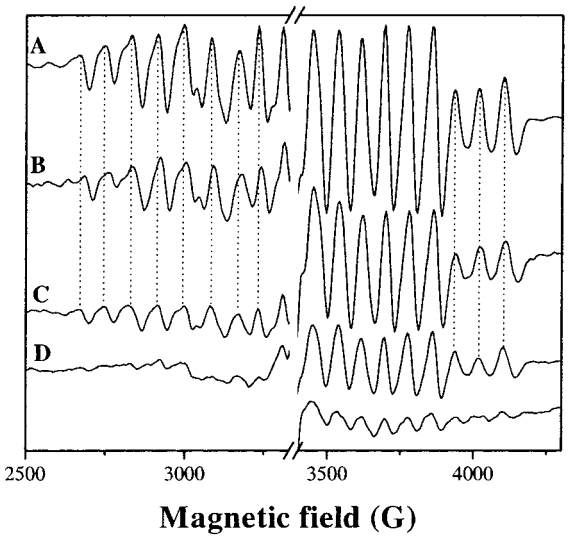

FIGURE 2: Effect of various solvents on the Mn(II)−Mn(III) multiline EPR signal, obtained after incubation for 18 h with 0.8 mM NO: (A) control sample, without solvent addition; (B) 1% methanol; (C) 1% DMSO; and (D) 1% ethanol. The contribution of the $Tyr_D^{\bullet}$ signal at $g = 2$ has been removed for clarity. EPR conditions: microwave frequency, 9.41 GHz; modulation amplitude, 25 G_{pp}; microwave power, 31 mW; temperature, 6 K.

positions, especially in the methanol-treated sample, at the low-field part of the spectrum. The solvents have a more dramatic effect on the signal amplitude. Methanol has the lowest-magnitude effect, decreasing the amplitude to ~60−65% of the control, while the signal is almost completely abolished by 1% ethanol. Addition of methanol after the reduction by NO caused a decrease of 30−40% (a decrease of 25% was reported in ref *22*). On the basis of this result, methanol was used as the solvent of choice for the P-p-BQ stock solution.

Figure 3 shows the EPR spectra recorded after flashing different but equivalent [displaying the same magnitude for the Mn(II)−Mn(III) signal] NO-reduced samples, containing 0.5 mM P-p-BQ and 1% methanol. The starting level of the Mn(II)−Mn(III) dimer is shown in Figure 3A. This spectrum was recorded following removal of NO and subsequent incubation at −30 °C for 30 min (*20*). After each EPR spectrum had been recorded, the illuminated samples were incubated at −30 °C for 30 min, and the amount of Mn(II)−Mn(III) signal was monitored (spectra not shown). This was reduced by 85−90% by the first flash and totally eliminated by subsequent flashes.

Inspection of the spectra in Figure 3 shows a pronounced S_2 multiline signal after the fourth flash (Figure 3E) (41% of the control in Figure 3I), with a small signal (13%) appearing after the second flash (Figure 3C). The S_2 multiline EPR signals observed after the fifth and sixth flashes (panels F and G of Figure 3, respectively) are expected to occur because of the photochemical miss factor. The level of the fifth flash (24% of the control S_2 and 59% of S_2 on the fourth flash) is consistent with a miss factor of ~12%. This miss factor would in part explain the appearance of the S_2 multiline on the sixth flash, with the remainder arising from those centers that displayed an S_2 multiline signal on the second flash.

Small, variable amounts of the S_2 multiline EPR signal at flashes 1−3 (panels B−D of Figure 3, respectively) were

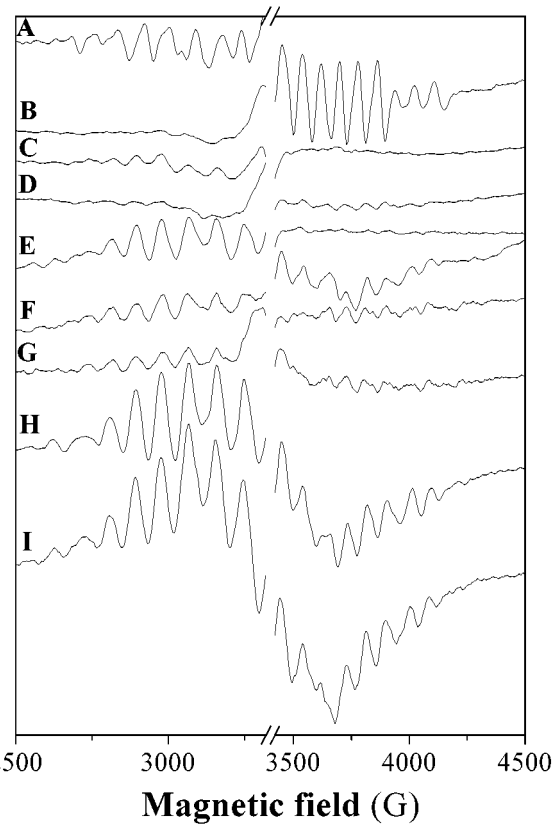

FIGURE 3: EPR spectra of different PSII samples treated with 0.8 mM NO for 18 h at −30 °C, in the presence of 0.5 mM P-p-BQ and 1% methanol: (A) level of the Mn(II)−Mn(III) multiline EPR signal representative of all samples, (B) one flash, (C) two flashes, (D) three flashes, (E) four flashes, (F) five flashes, (G) six flashes, (H) 200 K illumination of the sample at (E), following its dark adaptation for 5 h at 0 °C, and (I) S_2 multiline signal of an untreated control sample, containing 1% methanol and 0.5 mM P-p-BQ. Measurement temperature, 6 K for the Mn(II)−Mn(III) spectrum and 10 K for the S_2 signals. The contribution of the $Tyr_D^{\bullet}$ signal at $g = 2$ has been removed for clarity. Other EPR conditions are as described in the legend of Figure 2.

consistently observed. This may be indicative of a mixture of S states higher than the S_{-2} in the sample, at the point where the Mn(II)−Mn(III) EPR signal has reached a maximum. This may indicate that a non-negligible number of centers exists in less reduced states. Furthermore, if the decreased size of the Mn(II)−Mn(III) EPR signal in the presence of methanol is partly due to incompletely reduced centers, this would only enhance the effect. The S_2 multiline EPR signal in the two-flash samples appears to be bigger. It is possible that under the present conditions the S_0-to-S_{-1} reduction step is slow, compared to the S_1-to-S_0 or S_{-1}-to-S_{-2} step. This variation may be due to the decaying free NO concentration during the course of the −30 °C incubation (*22*).

To assess the maximum amount of S_2 signal that can be formed after the NO treatment, the sample illuminated with four flashes was further incubated for 5 h in the dark, at 10−15 °C, and then illuminated for 4 min at 200 K. This resulted in the S_2 multiline signal shown in Figure 3H. This spectrum is approximately 85% of that of the untreated control sample of Figure 3I, and it is somewhat bigger than that reported (60%) earlier (*22*). Similar levels of S_2 could be generated with the samples of Figure 3 that were flashed more than twice (i.e., those that were advanced to the S_0

level or higher by the flashes). The 85% yield of the S_2 signal generated by 200 K illumination indicates that the majority of centers function normally after the NO treatment, with a small decrease in intensity, corresponding to a loss of Mn from a small fraction of centers (see Experimental Procedures).

Tyrosine $_D^\bullet$ ($Tyr_D^\bullet$) was also monitored for each sample and for each flash. Under the experimental protocol described herein, the conversion of $Tyr_D^\bullet$ to the nitroso species described in ref *29* is not observed after the flash illumination. Given its redox relationship with the Mn cluster (*30*), a change in the amplitude of $Tyr_D^\bullet$ as a function of flash number would introduce a degree of uncertainty to the assignment of an S state to the NO-reduced state. Although the amount of $Tyr_D^\bullet$ present varied from sample to sample, no significant changes in the size of the $Tyr_D^\bullet$ EPR signal were observed in any of the samples before and after the train of flashes (not shown).

These EPR results are in agreement with the flash oxygen studies and indicate that the NO-reduced state corresponds to S_{-2}. Despite the fact that methanol was used as a solvent for the quinone, no S_0 spectrum was observed after the second flash. Given the small size of the S_0 signal, this could easily be hidden under the residual S_2 multiline signal (Figure 3C).

Flash Fluorescence Measurements. The S states modulate the chlorophyll fluorescence level (the F_o level). The S_0 and S_1 states are stronger quenchers of the F_o level than are the S_2 and S_3 states. As a consequence, a dampened period 4 oscillation is observed when the F_o is plotted as a function of flash number. Several authors have speculated about the cause of this S state-dependent quenching effect (*31*−*33*). This phenomenon provides another probe of the S state cycle, and we have used it to determine the S state generated by NO reduction.

In Figure 4, the results are summarized in three panels. In panel A, a control sample is compared with a NO-reduced sample. They both exhibit period 4 oscillations, and the fluorescence pattern of the NO-treated sample is shifted by three flashes relative to the control sample. Panel B shows that after one to three saturating preflashes (preflash frequency of 1 Hz) the fluorescence pattern downshifted by 1 with each preflash. Finally, panel C shows that when the time between the preflashes and the flash series is increased to 5 min (long enough for the S_2 state to decay back to S_1) there is very little difference between giving three and four preflashes. All three sets of experiments indicate that the samples were originally in the S_{-2} state.

Having samples that are largely in the S_{-2} state allows us to determine to what extent the S_{-1} and S_{-2} states quench the F_o level. However, on the first flash, an increase in the fluorescence level is observed (an *F* jump), which is unrelated to the modulating effect of the various S states. In the inset of Figure 5, the decay kinetics of this *F* jump are plotted. This is a "pump−probe" experiment; i.e., the effect of a saturating (pump) flash was determined at various times using a second (probe) flash. The decay curve can be fitted by two exponentials with decay times of 0.5 and 4.3 s, respectively, the fastest phase representing ~75% of the total. From this fit, the amplitude of the *F* jump can be calculated. By subtraction of the *F* jump from the fluorescence data, the quenching level of the S_{-2} state is made visible. The

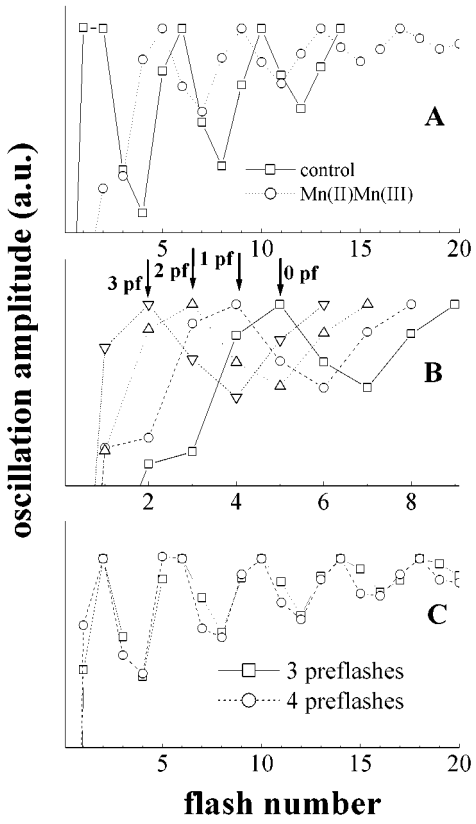

FIGURE 4: Period 4 oscillations of NO-reduced PSII samples. (A) Period 4 oscillations of a NO-treated sample compared with those of a control sample, (B) the shift of the period 4 oscillations by zero to three saturating preflashes at 1 Hz, and (C) comparison of the period 4 oscillations of NO-treated samples after three or four preflashes and a 5 min dark adaptation.

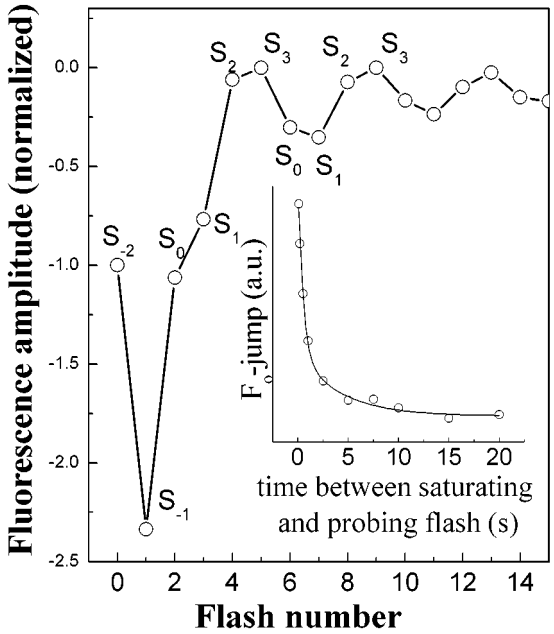

FIGURE 5: Chlorophyll *a* fluorescence period 4 oscillations of a sample in the Mn(II)−Mn(III) multiline state, after correction for the *F* jump on the first flash. The data were plotted on an arbitrary scale so that the S_0 and S_1 states equal approximately −1 and the S_2 and S_3 states equal approximately 0. The inset shows results of a pump−probe experiment to determine the decay kinetics of the *F* jump, on the basis of which the size of the *F* jump was calculated.

data are normalized in such a way that the S_0 and S_1 levels equal arbitrarily approximately −1. Figure 5 shows that the

quenching of the F_o level by the S_{-2} state is approximately equal to the quenching by the S_0 and S_1 states, whereas the quenching by the S_{-1} state is significantly stronger.

DISCUSSION

We have used three different methods to determine the dominant S state generated by reduction with NO. All of these studies indicated that the NO-induced state was an S_{-2} state, i.e., a state that is six redox equivalents below the state on which O_2 is evolved and three redox equivalents below the usual resting dark state (S_1). The O_2 electrode experiments were hampered by a high miss factor, by the inability to use an electron acceptor to make the comparison with the other techniques under identical conditions, and sometimes by a first-flash artifact that is probably caused by damaged centers. The preflash studies, however, provided strong support for the S_{-2} assignment. The fluorescence measurements suffered from the "*F* jump", the increase in fluorescence on the first flash, which we attribute to nonfunctional centers (see below). In addition, the influence of the reduced S states on the F_0 level remains unexplained. The oscillation patterns in the fluorescence levels were, however, clear, and preflash experiments again provided convincing support for the assignment of the reduced state as an S_{-2}. The EPR measurements benefited from the laser illumination and consequently the absence of a "double hit" factor. The EPR study, however, was hampered by the fact that the solvent used for the electron acceptor decreased the signal size and may have influenced the completeness of the reaction with NO. Despite these difficulties, the EPR study rather clearly and directly showed that the dominant state formed by NO reduction is four redox equivalents below the S_2 state, i.e., an S_{-2} state. Importantly, the EPR study allowed the other potential electron donors to be monitored, thereby eliminating some of the more obvious origins of an overestimate of the reduction level of the Mn cluster.

For all the fluorescence measurements, we observed an apparent increase in the *F* value that decayed on a time scale of seconds. Using a 10 Hz flash frequency, this jump of the *F* level was essentially limited to the first flash. The *F* jump decay (Figure 5, inset) can attributed (a) to charge recombination occurring in a small fraction of centers that have lost the Mn cluster during the NO incubation and pumping steps (as indicated by the presence of small amounts of free Mn^{2+} seen by EPR) and (b) possibly to any centers that remain unreduced by NO and that undergo $S_2Q_A^-$ recombination (*34*).

As stated in the Results, the mechanistic basis for the period 4-dependent quenching of the F_o level is unknown. The data in Figure 5 indicate that the S_{-1} state is the strongest quencher of F_o. It has been observed (*35*−*37*) that during the S_{-1}-to-S_0 transition, two protons are released. Given that protonation of the antenna system causes quenching of the S_0 level (*38* and references therein), and that the antenna system seems to affect proton release into the medium under some conditions (*39*), it may be worth considering whether the proton release may influence the fluorescence level. Clearly, a direct correlation between fluorescence and proton release does not exist (e.g., release of two protons on the S_3-to-S_0 step results in fluorescence quenching, while it results in a large increase in fluorescence on the S_{-1}-to-S_0 step). Speculation concerning these phenomena is premature, since the proton release measurements for the S_{-1}-to-S_0 step were performed using hydroxylamine rather than NO; in this work, we conclude that the two treatments appear to produce chemically different forms of the over-reduced S states. Proton measurements in NO-reduced PSII would be of interest in this regard.

An important conclusion from the flash O_2 measurements is that they show that NO-treated PSII is still capable of O_2 production and still follows a period 4 oscillation. The O_2 that was sometimes released on the first flash is unrelated to the NO-reduced state and is considered to be an artifact. The fact that it is eliminated by catalase points toward some kind of peroxide chemistry. A similar phenomenon has been observed before (*40* and references therein) and was related to the harshness of the treatment of the samples, and the possible presence of free manganese (*40*, *41*). The oxygen observed on the first flash may be related to damage to a small fraction of the centers, occurring at the NO pumping stage (EPR spectroscopy showed that a small amount of Mn^{2+} was invariably released during this procedure). The presence and size of this peak provided a means of evaluating the intactness of the sample after the NO treatment.

One rather peculiar property of the Mn(II)−Mn(III) EPR signal is that it is very sensitive to temperature. Above 0 °C, the signal very quickly disappears, only to be restored by a brief incubation at −30 °C (*20*). Under our experimental protocol, both the flash oxygen experiment and the EPR measurements had as the starting material PSII membranes that were characterized by the EPR-silent form of the NO-reduced state. The question then arises of whether the EPR-silent form is in an S state identical to the one yielding the Mn(II)−Mn(III) multiline signal. The change from the EPR-active form to the EPR-silent form is clearly reversible and is independent of the presence or absence of NO (*20*). Furthermore, there is no change in the oxidation state of PSII components that might react with the Mn cluster ($Tyr_D^{\bullet}$, cytochrome b_{559}). These observations rule out the possibility of a reversible oxidation−reduction process occurring during the EPR-active-to-EPR-silent conversion.

The incubation temperature of −30 °C was initially introduced in NO treatment protocols (*42*), because it slows the reactions with NO and protects against the over-reduction of the water-oxidizing enzyme. It was found that this temperature is very specific. Above −25 °C, the yield decreases dramatically. Lowering the temperature below −30 °C slows the reaction. A similar temperature dependence was found for the recovery of the Mn(II)−Mn(III) signal after the incubation at >0 °C. The recovery of the signal (in the absence of NO) requires a minimum of 30 min of incubation at −30 °C. This indicates some ordering process; the loss of the signal at high temperatures may be due to disordering. Alternatively, the loss of the signal could be due to a high-temperature-induced magnetic contact of the EPR-active dimer, the rest of the cluster forming a state with spread-out, very weak EPR signals. Related to the EPR-active-to-EPR-silent equilibrium are the effects of the various solvents discussed below.

The Mn(II)−Mn(III) multiline EPR signal also exhibits an organic solvent-dependent behavior, as is the case with the S_2 multiline EPR signal or the S_0 multiline signal (which appears only in the presence of methanol). The dramatic

change for the Mn(II)−Mn(III) signal is mostly on its size: from a decreased size (methanol and DMSO) to almost total disappearance, in the case of ethanol. The small shift of the multiline peaks is most pronounced on the low-field peaks in the presence of 1% methanol. We were also surprised by the fact that DMSO, probably the most benign of solvents used in PSII studies (at low concentrations, approximately 1%, it interferes in no observable way with the EPR signals of various PSII components), has such a pronounced effect on the amplitude of the Mn(II)−Mn(III) signal (Figure 3C). Although the possibility that this is in part due to incomplete reduction cannot be ruled out, we consider it more likely that these solvents are favoring the high-temperature (>0 °C) EPR-silent form of the cluster, as was discussed earlier for the case of methanol (*22*). Related probably to the effects of solvents is the observation that the Mn(II)−Mn(III) multiline signal in partially dehydrated samples used in the study of the orientation of the signal (*43*)[2] required a higher temperature of incubation with NO (−15 °C instead of −30 °C).

It has been reported that a relatively stable S_{-3} state can be produced by reduction of thylakoid membranes with hydrazine sulfate (*18*). The authors document the time dependence of the various S states produced during the reduction process. Since the reported levels of the S_{-2} state are quite substantial, both as a reduction intermediate and as a result of S_{-3} oxidation, we examined whether the S_{-2} multiline signal could be visible by hydrazine reduction. We were unable to detect such a signal, even following the seemingly necessary −30 °C incubation step. One important difference in the hydrazine reduction protocol (*18*) is the use of thylakoid membranes, rather than PSII-enriched membranes (we noticed, for instance, that during the incubation of PSII-enriched membranes with hydrazine, substantial amounts of Mn^{2+} were released). It may be possible that the hydrazine reduction is more unspecific, resulting in an S_{-2} state, which is not characterized by an isolated Mn(II)−Mn(III) dimer. A qualitative difference in the end result of the Mn cluster reduction using different reductants (hydroxylamine, hydrazine, and hydroquinone) has been reported elsewhere, e.g., in ref *19*, where it is postulated that there may be different valence distributions for the S_{-1} state, and in ref *44*, where the S_{-3} state obtained by hydroxylamine reduction is unstable.

It would be interesting to speculate about the valence mixture of the four Mn ions in each of the S states, based on the presence of a Mn(II)−Mn(III) dimer in the S_{-2} state, which can be converted with a high quantum yield to higher S states. For the S_1 state, it has been proposed that the valence distribution of the tetramer is Mn(III)Mn(III)Mn(IV)Mn(IV), based on EXAFS (*45*, *46*) or EPR data (*47*, *48*), or Mn(III)-Mn(III)Mn(III)Mn(III) (*49*), based on a simulation of the S_2 multiline EPR signal (for a recent review, see ref *50*). This would mean that the S_{-2} state is either Mn(II)Mn(III)-Mn(III)Mn(III) or Mn(II)Mn(III)Mn(II)Mn(II), respectively. If the latter case were true, then the S_{-2} state would probably be the lowest stable S state that can be attained, before all the Mn ions are reduced to Mn^{2+} and the cluster disintegrates. However, an S_{-3} state, which is relatively stable, has been described previously (*18*). A 2Mn(III)−2Mn(IV) distribution is therefore more consistent for the S_1 state (for a discussion, see also ref *51*).

A specific, S_{-2} state is now assigned to the Mn(II)−Mn(III) dimer. S_{-2} in our studies appears in two forms, which are in temperature equilibrium: an EPR-active form (developing at −30 °C) and an EPR-silent form (brief incubation of the EPR-active form at >0 °C). If Mn oxidation is assumed during the S_{-2}-to-S_{-1} and S_{-1}-to-S_0 steps, S_{-2} in its EPR-silent form should be a half-integer. An interesting goal would be to find the proper conditions for detection of the EPR signature of the silent form. This would provide important information about the "invisible" part of the Mn cluster. If these ions could be detected, then this could be important in resolving the long-standing question of the redox states of the Mn ions in the Mn cluster during the S state cycle. Future research will focus on this question. These studies will potentially provide useful insights into not only the progressive changes that occur as the cluster advances to the higher oxidation states but also the assembly process of the cluster.

ACKNOWLEDGMENT

G.S. thanks Josephine Sarrou for providing some of the NO-treated samples. Ch.G. thanks Peter Faller and Nikos Ioannidis for useful discussions, Alain Boussac for his help with the laser, and Guillaume Voyard for constructing the pumping station.

REFERENCES

1. Debus, R. J. (1992) *Biochim. Biophys. Acta 1102*, 269.
2. Yachandra, V. K., Sauer, K., and Klein, M. P. (1996) *Chem. Rev. 96*, 2927.
3. Roelofs, T. A., Liang, W., Latimer, M. J., Cinco, R. M., Rompel, A., Andrews, J. C., Sauer, K., Yachandra, V. K., and Klein, M. P. (1996) *Proc. Natl. Acad. Sci. U.S.A. 93*, 3335.
4. Iuzzolino, L., Dittmer, J., Meyer-Klaucke, W., and Dau, H. (1998) *Biochemistry 37*, 17112.
5. Dismukes, G. C., and Siderer, Y. (1981) *Proc. Natl. Acad. Sci. U.S.A. 78*, 274.
6. Casey, J. L., and Sauer, K. (1984) *Biochim. Biophys. Acta 767*, 21.
7. Zimmermann, J.-L., and Rutherford, A. W. (1984) *Biochim. Biophys. Acta 767*, 160.
8. Boussac, A., Girerd, J.-J., and Rutherford, A. W. (1996) *Biochemistry 35*, 6484.
9. Haddy, A., Durnham, W. R., Sands, R. H., and Aasa, R. (1992) *Biochim. Biophys. Acta 1099*, 25.
10. Boussac, A., and Rutherford, A. W. (2000) *Biochim. Biophys. Acta 1457*, 145.
11. Messinger, J., Nugent, J. H. A., and Evans, M. C. W. (1997) *Biochemistry 36*, 11055.
12. Ahrling, K. A., Peterson, S., and Styring, S. (1997) *Biochemistry 36*, 13148.
13. Messinger, J., Robblee, J. H., Wa, O. Y., Sauer, K., Yachandra, V. K., and Klein, M. P. (1997) *J. Am. Chem. Soc. 119*, 11349.
14. Matsukawa, T., Mino, H., Yoneda, D., and Kawamori, A. (1999) *Biochemistry 38*, 4072.
15. Ioannidis, N., and Petrouleas, V. (2000) *Biochemistry 39*, 5246.
16. Tamura, N., and Cheniae, G. M. (1987) *Biochim. Biophys. Acta 890*, 179.
17. Ananyev, G. M., Zaltsman, L., Vasko, G. C., and Dismukes, G. C. (2001) *Biochim. Biophys. Acta 1503*, 52.
18. Messinger, J., Seaton, G., Wydrzynski, T., Wacker, U., and Renger, G. (1997) *Biochemistry 36*, 6862.

[2] The values of $A_{||}$ have been misquoted in the caption of Figure 1 of this reference, due to an arithmetic error. The correct values are as follows: for Mn(II), $A_{||} = -691$ MHz (instead of −762 MHz); and for Mn(III), $A_{||} = -207$ MHz (instead of −200 MHz).

19. Mei, R., and Yocum, C. F. (1992) *Biochemistry 31*, 8449.
20. Goussias, Ch., Ioannidis, N., and Petrouleas, V. (1997) *Biochemistry 36*, 9261.
21. Sarrou, J., Ioannidis, N., Deligiannakis, Y., and Petrouleas, V. (1998) *Biochemistry 37*, 9261.
22. Ioannidis, N., Sarrou, J., Schansker, G., and Petrouleas, V. (1998) *Biochemistry 37*, 16445.
23. Ioannidis, N., Schansker, G., Barynin, V. V., and Petrouleas, V. (2000) *J. Biol. Inorg. Chem. 5*, 354.
24. Berthold, D. A., Babcock, G. T., and Yocum, C. F. (1981) *FEBS Lett. 134*, 231.
25. Ford, R. C., and Evans, M. C. W. (1983) *FEBS Lett. 160*, 159.
26. Kramer, D. M., Robinson, H. R., and Crofts, A. R. (1990) *Photosynth. Res. 26*, 181.
27. Kurreck, J., Schoedel, R., and Renger, G. (2000) *Photosynth. Res. 63*, 171.
28. Zimmermann, J.-L., and Rutherford, A. W. (1986) *Biochemistry 25*, 4609.
29. Sanakis, Y., Goussias, Ch., Mason, R. P., and Petrouleas, V. (1997) *Biochemistry 36*, 1411.
30. Styring, S., and Rutherford, A. W. (1987) *Biochemistry 26*, 2401.
31. Shinkarev, V. P., Xu, C., Govindjee, and Wraight, C. A. (1997) *Photosynth. Res. 51*, 43.
32. Delrieu, M. J. (1998) *Biochim. Biophys. Acta 1363*, 157.
33. Putrenko, I., Vasil'ev, S., and Bruce, D. (1999) *Biochemistry 38*, 10632.
34. Lavergne, J. (1991) *Biochim. Biophys. Acta 1060*, 175.
35. Saygin, Ö., and Witt, H. T. (1985) *FEBS Lett. 808*, 123.
36. Förster, V., and Junge, W. (1985) *Photochem. Photobiol. 41*, 191.
37. Haumann, M., and Junge, W. (1996) in *Oxygenic Photosynthesis: The Light Reactions* (Ort, D. R., and Yocum, C. F., Eds.) Advances in Photosynthesis, Vol. 4, p 165, Kluwer Academic Publishers, Dordrecht, The Netherlands.
38. Horton, P., Ruban, A. V., and Walters, R. G. (1996) *Annu. Rev. Plant Physiol. Plant Mol. Biol. 47*, 655.
39. Jahns, P., and Junge, W. (1992) *Biochemistry 31*, 7398.
40. Taoka, S., Jursinic, P. A., and Seibert, M. (1993) *Photosynth. Res. 38*, 425.
41. Berg, S. P., and Seibert, M. (1987) in *Progress in Photosynthesis Research* (Biggins, J., Ed.) Vol. 1, p 589, Martinus Nijhoff Publishers, Dordrecht, The Netherlands.
42. Goussias, Ch., Sanakis, Y., and Petrouleas, V. (1995) in *Photosynthesis: from Light to Biosphere* (Mathis, P., Ed.) Vol. 1, p 835, Kluwer Academic Publishers, Dordrecht, The Netherlands.
43. Hanley, J., Sarrou, J., and Petrouleas, V. (2000) *Biochemistry 39*, 15441.
44. Beck, W. F., and Brudvig, G. W. (1987) *Biochemistry 26*, 8285.
45. Riggs, P. J., Mei, R., Yocum, C. F., and Penner-Hahn, J. E. (1992) *J. Am. Chem. Soc. 114*, 10650.
46. Ono, T. A., Noguchi, T., Inoue, Y., Kusunoki, M., Matsushiata, T., and Oyanagi, H. (1992) *Science 258*, 1335.
47. Hasegawa, K., Kusunoki, M., Inoue, Y., and Ono, T. (1998) *Biochemistry 37*, 9457.
48. Peloquin, J. M., Campbell, K. A., Randall, D. W., Evanchik, M. A., Pecoraro, V. L., Armstrong, W. H., and Britt, R. D. (2000) *J. Am. Chem. Soc. 122*, 10926.
49. Zheng, M., and Dismukes, G. C. (1996) *Inorg. Chem. 35*, 3307.
50. Carrell, T. G., Tyryshkin, A. M., and Dismukes, G. C. (2002) *J. Biol. Inorg. Chem. 7*, 2.
51. Messinger, J. (2000) *Biochim. Biophys. Acta 1459*, 481.

BI015903Z